Piezoelectric properties of PbTiO(3) thin films characterized with piezoresponse force and high resolution transmission electron microscopy

Morelli, A.; Venkatesan, Sriram; Kooi, B. J.; Palasantzas, G.; De Hosson, J. Th. M.

Published in:
Journal of Applied Physics

DOI:
10.1063/1.3088913

Publication date:
2009

Piezoelectric properties of $PbTiO_3$ thin films characterized with piezoresponse force and high resolution transmission electron microscopy

A. Morelli, Sriram Venkatesan, B. J. Kooi, G. Palasantzas,[a] and J. Th. M. De Hosson
Department of Applied Physics, Zernike Institute for Advanced Materials and Netherlands Institute for Metals Research, University of Groningen, Nijenborgh 4, 9747 AG Groningen, The Netherlands

(Received 22 September 2008; accepted 24 January 2009; published online 19 March 2009)

In this paper we investigate the piezoelectric properties of $PbTiO_3$ thin films grown by pulsed laser deposition with piezoresponse force microscopy and transmission electron microscopy. The as-grown films exhibit an upward polarization, inhomogeneous distribution of piezoelectric characteristics concerning local coercive fields, and piezoelectric coefficient. In fact, the data obtained reveal imprints during piezoresponse force microscopy measurements, nonlinearity in the piezoelectric deformation, and limited polarization reversal. Moreover, transmission electron microscopy shows the presence of defects near the film/substrate interface, which can be associated with the variations of piezoelectric properties. © *2009 American Institute of Physics*.
[DOI: 10.1063/1.3088913]

I. INTRODUCTION

Ferroelectric thin films of today are subject of high technological interest because of important applications, i.e., in electromechanical transducers, accelerometers, micropositioners, etc., and their promising use for nonvolatile memories.[1,2] The quest for miniaturization has given a strong impetus to nanoscale investigation of the quantitative properties, polarization domain engineering, and domain dynamics. In particular, over the last decade piezoresponse force microscopy (PFM) has been proven a powerful technique for ferroelectric films characterization at a nanoscale level.[3]

Although characterization with PFM has been extensively performed for $Pb(Zr,Ti)O_3$ (PZT) films,[4,5] experimental data of nanoscale variations of physical properties of $PbTiO_3$ (PTO) films are still lacking. In fact, reported data on PTO films processed from modified alkoxide solution precursors showed a piezoelectric coefficient value $d_{33} \approx 65$ pm/V.[6] Moreover, the d_{33} hysteresis curves gave evidence of the presence of a weak imprint, and d_{33} exhibited nonlinear behavior with increasing amplitude of the applied ac electric field used in PFM.[6] Although, the observed nonlinearity was attributed to possible domain wall motion, its origin requires further investigation since detailed knowledge of the piezoelectric behavior of PTO films is necessary in applications. In addition, for epitaxially grown PTO films on MgO substrates[7] with pulsed laser deposition having also *a* domains (which were switching under the influence of external field), d_{33} values $\sim 20-80$ pm/V were reported for film thicknesses of 60–200 nm.

Furthermore, retention loss is a vital problem for nonvolatile memories applications. As reported for PZT granular films the process starts by thermal activation, eventually after a latent period,[8] at domain boundaries and proceeds via lateral expansion of the reversed portion. The latter can be fitted by a stretched exponential $\sim 1-\exp(-ct^d)$ with exponent $d<1$.[9] Retention loss studies on PTO films grown by hydrothermal epitaxy show a long latent period (~ 1470 h) after which the loss depends on the size of written domain.[8] The latter can be explained by instability of curved c^+/c^- domain walls due to the presence of head-on polarization. However, in the case of leakage currents the retention loss took place rather fast with a characteristic time of less than 1 h.[10] Moreover, this process was characterized by a stretched exponential with exponent $d>1$, which it is clearly distinct from that related to retention loss due to grain boundary effects.[10] Therefore, in this paper we will present investigations of the nonlinear behavior for single domain PTO films (in absence of *a* domains to avoid complications due to their switching by the electric field of the PFM tip). Our study is performed in terms of combined PFM and transmission electron microscopy (TEM) characterization of ferroelectric domain structure and film/substrate interfaces. In addition, TEM analysis shows images of defects at the interfaces for both films and therefore we focused on functional properties by PFM. As a result the quality of the film substrate interface and its impact on the ferroelectric functionality will be explored in detail. In fact, the piezoelectric coefficient d_{33} (which is the major functional property since the as deposited films have only *c* domains), the imprint behavior, and coercive fields will be used for comparison and appropriate evaluation of the functional properties of ferroelectric materials. In addition, special attention will be paid on retention loss characteristics in combination with any nonlinear piezoresponse and imprint effects.

II. EXPERIMENTAL PROCEDURE

The specimens under study are $PbTiO_3$ thin films grown by pulsed laser deposition (PLD), on (001) $SrTiO_3$ (STO) substrates, with an intermediate layer of $SrRuO_3$ (SRO) acting as bottom electrode; specifically the sample studied extensively (termed *A*1) is 130 nm PTO/50nm SRO/STO film, while for comparison of nanoscale piezoresponse characteristics another sample, (termed *A*2) 120 nm PTO/40nm

[a]Author to whom correspondence should be addressed. Electronic mail: g.palasantzas@rug.nl.

SRO/on STO substrate, was used. For the structural characterization of the PTO films a JEOL 2010F TEM was employed operating at 200 kV. TEM analyses were performed in PTO cross-section samples. The specimens were mechanically thinned by cutting, grinding, polishing, dimpling, and finally ion milling using a precision ion polishing system (Gatan model 691) with 4 kV Ar^+ ions at an incident angle of 8°.

Furthermore, a commercial scanning probe microscope (Dimension 3100, Nanoscope IIIa, Veeco Instruments) was used for the PFM measurements. A lock-in amplifier (SR830, Stanford Research) was employed for simultaneous piezoresponse phase and amplitude (PR phase and PR amplitude) acquisition. The measurements were performed with conductive Sb doped Si tip cantilever (TESP-Veeco Instruments) with nominal spring constant 42 N/m and resonance frequency ~300 kHz. The tip has an initial radius of curvature $R_{ROC} \sim 10$ nm, which increases up to 50 nm after various PFM measurements due to local wear out by operating in contact mode. Typical applied contact forces were $F_c \sim 0.8\ \mu N - 1.2\ \mu N$. These forces are sufficiently weak to avoid any significant local depolarization, but sufficiently high to ensure a proper contact to minimize electrostatic contributions on the PFM signal.[11]

PR phase images of domains were acquired in scanning mode, with a typical modulation ac signal frequency 5 kHz and amplitude $V_{ac}=1.5$ V. The piezoelectric constant d_{33} is the longitudinal coefficient of the transposed piezoelectric tensor. If the axis normal to the sample surface is the z axis, d_{33} relates the strain (associated to shape changes) and applied electric field (or voltage modulation signal V_{ac} between tip and grounded sample) along this axis. Therefore, the measurement of d_{33} was performed by ramping V_{ac} and acquiring at each step the PR phase and PR amplitude.[12] The slope of the PR amplitude vs V_{ac} plot gives d_{33} as long as any nonlinear behavior is absent so that any offset error is excluded by the measurement. Local hysteresis loops were measured in pulse mode. After applying a dc bias pulse (from 0.2 to 1 s) and a typical waiting time of 0.1 s, PR phase and PR amplitude data were acquired simultaneously. For each bias step the V_{ac} was ramped between 0.5 and 2.5 V (in steps of 0.5 V) and an acquisition time of 0.2 s was used to perform the d_{33} measurement for each applied dc field. The pulsed voltage was cycled in both cases values ranging from −10 to +10 V. For the typical hysteresis loop measurements, the piezoresponse is defined as d_{33} cos(PR phase).

III. RESULTS AND DISCUSSION

PR phase imaging of the as deposited films shows a monodomain with polarization normal to the surface and upward direction (c^+ domain). Domains with polarization parallel to the surface (*a* domains) were not detected by PFM and, if present, they have a lateral size less than the tip radius ~10–20 nm. In addition, TEM measurements confirmed the absence of *a* domains. Furthermore, domain reversal was performed by applying dc bias voltages of 3.5–4 V. It was applied from the tip at a scanning speed of 1 Hz over a $1 \times 1\ \mu m^2$ area in order to obtain a square *c* domain with

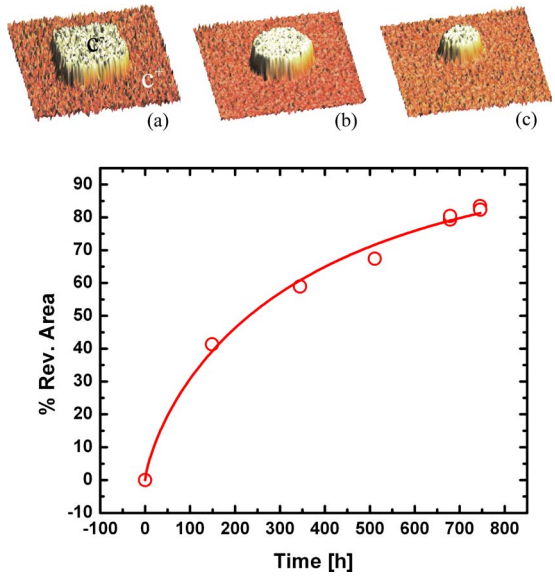

FIG. 1. (Color online) PR phase images acquired after polarization reversal: (a) after poling, (b) 345 h, and (c) 745 h later for sample *A*1. (d) Plot of area percentage as a function of time evaluated by PR phase images taken after polarization reversal over a 1 μm^2 area by poling the tip at 3.5 V.

reversed polarization (downward or a c^- domain, Fig. 1). Indeed, Fig. 1 shows retention loss measurements for more than 750 h. The figure shows that a latent period is not present and that the back-switched area can be fitted by a stretched exponential of the form $A_{r\text{-area}} \sim 1 - \exp[-(t/k)^d]$, with *k* a characteristic retention loss time. Indeed, $A_{r\text{-area}}$ is the ratio of the back-switched area and the initial area of predetermined polarization direction.

The PR phase images for calculating the back-switched area were obtained with $V_{ac}=1.5$ *V*, which is low enough not to enhance the retention loss. The fitting gave the exponents $d=0.75\pm0.06$. The effective inversion time was $k=376\pm15$ h. Despite differences, these values are comparable to retention loss times obtained in other studies for PTO films grown on STO (Nb doped) substrates.[8] From the results it can be inferred that the retention loss occurs by a random walk process since $d<1$, which is generated by the c^+/c^- domain wall lateral movement. As pointed out in Ref. 13, this is caused by the poling procedure (initial domain reversal) of the PFM tip that generates curved domains with walls not parallel to the polarization vector leading to a head-to-head polarization configuration. This produces uncompensated positive charges at the curved c^+/c^- domain wall, since the films are not leaky (absence of leakage currents through the film) as our Conductive AFM studies indicated,[10] resulting in depolarization fields with upward direction.

A. TEM characterization and analysis

The samples analyzed by PFM were also imaged using TEM to unravel any possible disorder at the film substrate interface. Figure 2 shows a cross sectional bright field image for the *A*1 sample. At room temperature the PTO film has a tetragonal structure with $a=b=3.899$ Å and $c=4.154$ Å.[14] The SRO is a transition-metal oxide with a metallic conductivity and orthorhombic structure with lattice constants *a*

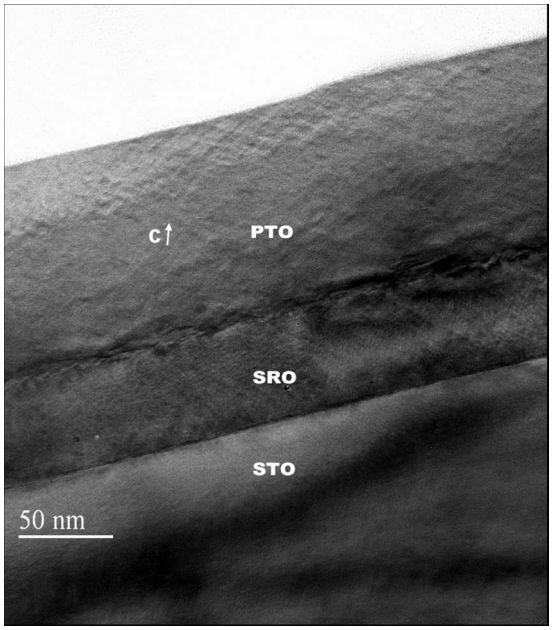

FIG. 2. Bright field TEM image of the *A*1 PTO sample, which shows the presence of defects at the electrode-film interface.

=5.567 Å, b=5.530 Å, and c=7.844 Å,[15,16] which is often viewed as a tetragonal structure with $a=b=3.93$ Å and $c=7.85$ Å or a two-stacked pseudocubic perovskite unit cell with $a=3.93$ Å. The STO has a cubic structure with lattice constant of 3.905 Å. These crystallographic data indicate the presence of misfit strain at the interfaces. The TEM images show clearly that the PTO film is completely c-axis oriented without any a domains, which was also confirmed using x-ray diffraction[17] and it is in agreement with the claim previously from our PFM studies regarding the absence of a domains.

In addition, the PTO/SRO interface shows nonuniformities. The contrast these defects generate extends up to a few monolayers away from the interface as is clearly observed in the high resolution TEM images of Fig. 3. On the other hand, the SRO/STO interface is characterized by a sharp interface, which demonstrates a perfect coherent epitaxial matching (Fig. 3). TEM analysis of sample *A*2 gave also similar results. The lack of coherency between PTO and SRO films can be attributed to the existing misfit strain. The in-plane lattice mismatch between SRO and PTO at room temperature is ~0.9% which is larger than the one at the substrate-electrode interface of ~0.6%. However, it is still more likely that the origin of the defects is related to the surface condition of the SRO bottom electrode prior to the PTO film deposition. This is because the SRO surface is exposed shortly to air and stored under vacuum prior to PTO deposition. Note that with optimal surface conditions it turned out possible to grow a defect-free film.[16,17]

B. Piezoelectric coefficient analysis

In order to gain more insight into the influence of interfaces onto the PTO film functionality, we performed detailed PFM studies. Figure 4(a) shows the V_{ac} dependence of the partial d_{33}^{p}=PR amplitude/V_{ac} and of the PR phase (inset)

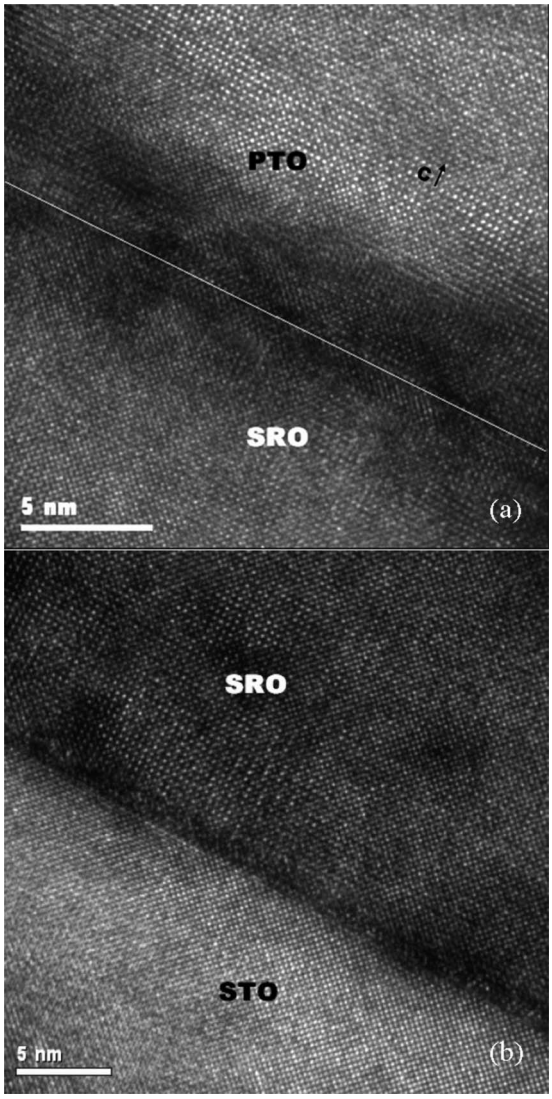

FIG. 3. High resolution TEM images of *A*1 showing (a) nonuniformities and defects at the electrode-film interface and (b) sharp interface of substrate-electrode without defects.

for c^{+} and c^{-} domains over an area on sample *A*1. The partial d_{33}^{p} values are relatively constant below a voltage $V^{*}\approx 2.5$ V, while they increase significantly for voltages $V_{ac}>V^{*}$. For this reason the actual piezoelectric constant d_{33} is finally calculated in the range 0.5–2.5 V by the slope of the PR amplitude vs V_{ac} plot for higher accuracy giving $d_{33}=21.2\pm0.5$ and 25.6 ± 0.4 pm/V for c^{+} and c^{-} domains, respectively. Nonetheless, the piezoelectric constants show a significant spatial variation in the range $d_{33}\sim10-30$ pm/V over the area of the film. Moreover, Fig. 4(b) shows the V_{ac} dependence of the partial d_{33}^{p} values and the PR phase for sample *A*2 (inset). The piezoresponse over the c^{-} domain gives an initial d_{33}^{p} smaller than that for c^{+}, but the nonlinearity is much more pronounced for the c^{-} domain for $V_{ac}>V^{*}$. The obtained d_{33} values (for $V_{ac}<V^{*}$) from the linear fit are $d_{33}=35.89\pm0.68$ pm/V for the c^{+} and $d_{33}=32.57\pm0.47$ pm/V for c^{-} domains. In addition, these values vary over the film surface in the range $d_{33}\sim20-40$ pm/V.

Although in literature the main source of nonlinearity is supposed to be 90° domain wall motion,[6,18–20] for the PTO

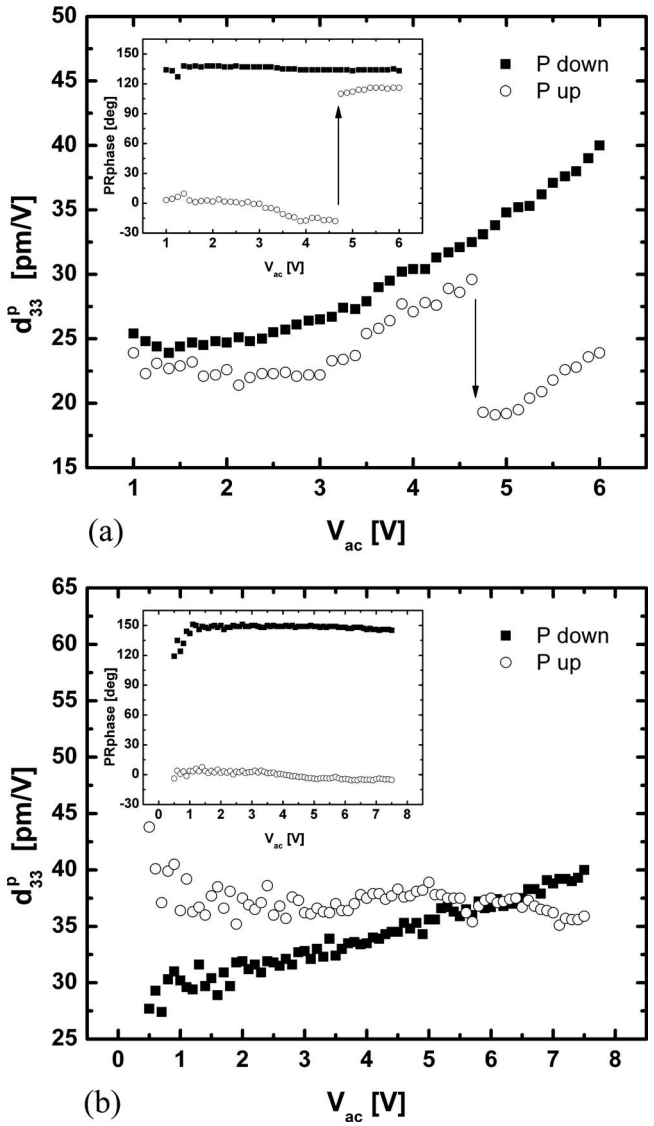

FIG. 4. Partial d_{33}^{p} vs amplitude of the modulation voltage (a) for sample *A*1 and (b) for sample *A*2. Insets show the PR phase vs amplitude for the modulation voltage. Arrows in (a) indicate qualitatively the position of polarization reversal.

films under investigation such domains were not detected as it was confirmed by TEM and x-ray diffraction. Therefore, the presence of such a kind of domain walls can be excluded as the source of the nonlinearity. For both samples the obtained piezoelectric values are comparable to the ones reported in literature (and obtained by PFM).[7] Although these values are lower than those obtained with laser interferometry,[6] they can become comparable if the clamping effect is also taken into account.[21] In fact, due to inhomogeneity of the electric field of the PFM tip, the piezoelectric deformation during PFM measurements occurs only within a small volume of the sample confined underneath the tip. Clamping of this volume by the rest of the sample results in reduced piezoelectric deformation. Moreover, Fig. 4(a) indicates that the response over the c^{+} domain in sample *A*1 gives initially a partial d_{33}^{p} smaller than that for the c^{-} domain and in addition a drop occurs for $V_{\mathrm{th}} \approx 4.5$ *V*. Simultaneously the polarization changes direction since the PR phase increases by about 140°. Such a phenomenon occurred only over certain areas of the film and polarization inversion took place also for c^{-} domains. In fact, the polarization inversion with increasing V_{ac} has already been reported in Refs. 18 and 22. It was explained by the presence of hidden 180° domain walls below the film surface, consisting of two layers of opposite polarization. When the V_{ac} generates a field strong enough at the wall position, it would be depinned. Given the inhomogenous field generated in the film by the PFM tip, moving towards the zone where the field is stronger, i.e., towards the tip, the domain of reverse polarization (close to the film/substrate interface) will expand through the whole film thickness. Thus, in Fig. 4(a) where the inversion occurs, the bottom layer would be a c^{-} domain, which under increasing V_{ac}, expands until it reaches the top surface of the film. In Ref. 18 the domain wall was generated during the writing operation (polarization reversal) and the created domain did not reach the bottom of the film. In our case we have both types, i.e, inversion of a written domain and a domain in the as deposited films. Since the inversion polarization takes place only in some areas and the TEM images (Figs. 2 and 3) indicate interface disorder, it is likely that a domain wall is generated by charge trapping caused by the presence of the interface defects. In fact, in the case that the defects are located not exactly at the interface but in its proximity inside the PTO film, trapped charges can give rise to depolarizing fields of opposite direction below and above the domain wall. Therefore, the inhomogeneity due to the presence of interface defects can be a plausible explanation why the d_{33}^{p} shows different behaviors at different areas. The fact that the inversion is recorded for both c^{+} and c^{-} domains, it is interpreted as the result of charges of different signs trapped within defects inside the PTO film. In fact, as schematically represented in Fig. 5, the PTO volume between defects and the interface experiences a high permanent electric field. The latter can be strong enough to influence the polarization configuration. Therefore two polarization layers are present in the as deposited film where the trapped charges are positive [Fig. 5(a)]. In a similar manner two layers are created when reversing the polarization over an area below which negative charges are trapped in defects [Fig. 5(b)]. As already reported in Refs. 18 and 22, increasing the ac voltage during reading could depin the domain wall resulting in expansion of the domain at the bottom of the film through the whole thickness [Fig. 5(c)]. Note that as reported in Ref. 18, before inversion the partial d_{33}^{p} decreases to zero since the expanding bottom layer domain responds equivalently (having opposite phase) at some V_{ac} with the top layer. However, in our measurements the responses of the c^{+} and c^{-} domains do not show this behavior.

C. Hysteresis loop analysis

Finally, piezoresponse hysteresis loops, as it is shown in Fig. 6, confirmed again the ferroelectric behavior of the films under study, while it showed pronounced imprint. Following our previous discussion about the piezoelectric coefficient d_{33}, the piezoresponse that is plotted in Fig. 6 is defined as $d_{33}\cos(\mathrm{PR\ phase})$. Defining the forward and reverse coercive biases as the two points, V^{+} and V^{-}, where the piezoresponse

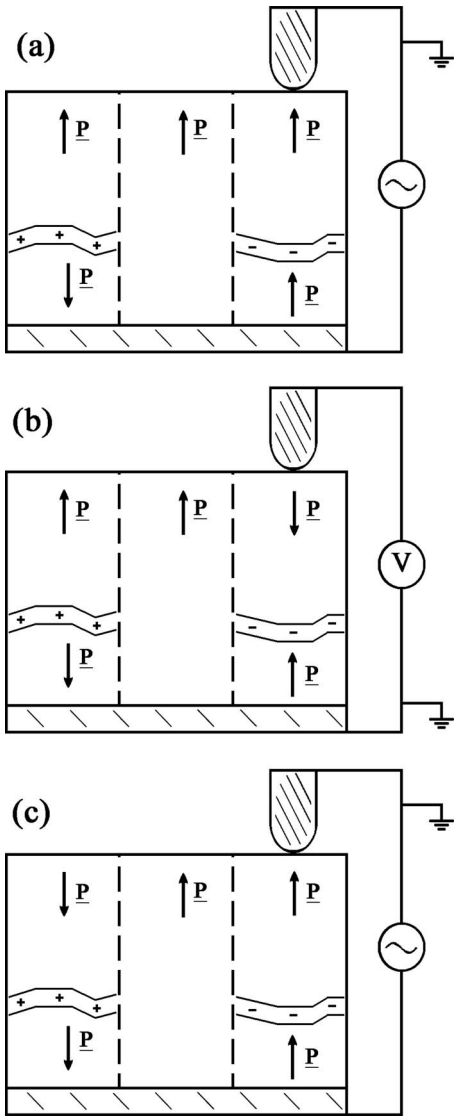

FIG. 5. Diagram of the domain configuration in the film. (a) The as-grown film surface shows a c^+ monodomain independent of defects close to the bottom electrode. In this case three different volumes are represented from left to right: volume with positive defect charges, volume without defects, and volume with negative defect charges. In (b) the polarization is reverted in the volume with negative charges. As a result two layers of polarization configurations are present within the volume with negative defects. If we scan the surface with increasing modulation voltage as in (c), the latter triggers polarization back switching by expansion of the bottom polarization layer.

is zero, the imprint Im, if present, can be defined as $\mathrm{Im}=(V^+ + V^-)/2$ and the average coercive bias as $V_c=(|V^+| + |V^-|)/2$.[23] For the measurement in Fig. 6 regarding sample *A*1 the imprint is Im=−1 *V* and the coercive bias V_c =3.6 *V*. However, these values vary over the sample surface with Im varying from about ~−1.7–+1.5 V and V_c between ~1.5 and 6 V. In addition, for sample *A*2 the hysteresis in Fig. 6 gave Im=−0.63 V and coercive bias V_c=4.9 V. For this sample, the imprint Im varies in the range ~−1.6–+0.5 *V* over the film surface and V_c between ~3.5 and 4.9 V. The imprint Im is comparable to imprint values of ~1 V for PTO films in former studies.[24] It can be explained by the different work functions of the bottom SRO electrode and of the Si doped PFM tip acting as top electrode[25,26] and/or by

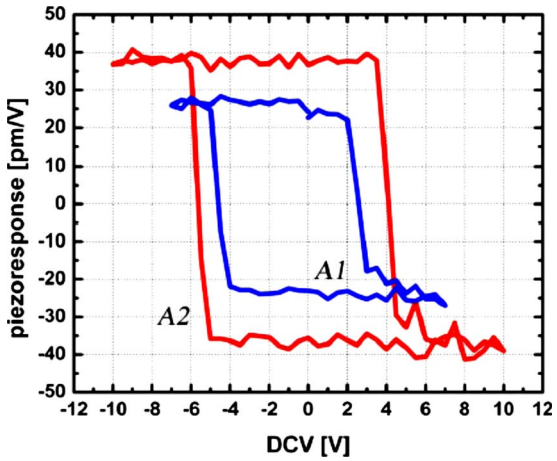

FIG. 6. (Color online) Piezoelectric hysteresis loop of sample *A*1 (blue line) and *A*2 (red line), performed in pulse mode with pulse time 0.2 s, settling time 0.1 s, and acquisition time 0.2 s, with modulation frequency 5 kHz. The vertical axis is the piezoresponse=d_{33} cos(PR phase).

the presence of a depolarizing field caused by charge redistribution due to interface disorder (Figs. 2 and 3). The obtained parameters from the hysteresis loops indicate that the films have significant ferroelectric properties, however, with significant variation at nanoscales.

IV. CONCLUSIONS

We studied the functionality of PTO samples grown by PLD on SRO electrodes by means of combined TEM and PFM techniques. The TEM images show the presence of defects at the electrode/film interface and confirm the absence of *a* domains. The presence of defects influences retention, homogeneity of piezoelectric characteristics over the surface, and it could be a competing factor in the polarization inversion under increasing modulation amplitude V_{ac} during PFM measurements of the d_{33} coefficient. An important finding in our work is that the nonlinearity in the PR amplitude vs V_{ac} cannot be attributed to 90° domain walls movement as it was indicated in former studies, since this type of walls was absent in the studied PTO films.[27] Retention longer than 1 month was shown with a loss prompted by c^+/c^- domain wall movement. The obtained d_{33} values of 30–40 pm/V were comparable to values reported in literature. Finally, as a reasonable statement concerning the film functionality, we can infer that they possess useful ferroelectric properties despite the nanoscale variation of d_{33} over the film surface and the relatively weak imprint found by hysteresis measurements.

ACKNOWLEDGEMENTS

We would like to acknowledge support by the Zernike Institute for Advanced Materials through the MSC +program. We thank A. Vlooswijk and B. Noheda for providing the PTO samples and P. van Loosdrecht for providing the lock-in amplifier that was used for the PFM measurements.

[1]J. F. Scott, Ferroelectr. Rev. **1**, 1 (1998).
[2]R. Ramesh, S. Aggarwal, and O. Auciello, Mater. Sci. Eng. **32**, 191 (2001).
[3]A. L. Kholkin, S. V. Kalinin, A. Roelofs, and A. Gruverman, in *Scanning Probe Microscopy: Electrical and Electromechanical Phenomena at the Nanoscale*, edited S. V. Kalinin and A. Gruverman (Springer, New York, 2007), pp. 173–214.
[4]A. L. Kholkin, V. V. Shvartsman, D. A. Kiselev, and I. K. Bdikin, Ferroelectrics **341**, 3 (2006).
[5]V. Nagarajan, A. Roytburd, A. Stanishevsky, S. Prasertchoung, T. Zhao, L. Chen, J. Melngailis, O. Auciello, and R. Ramesh, Nature Mater. **2**, 43 (2003).
[6]Z. Kighelman, D. Damjanovic, M. Cantoni, and N. Setter, J. Appl. Phys. **91**, 1495 (2002).
[7]Y. K. Kim, S. S. Kim, H. Shin, and S. Baik, Appl. Phys. Lett. **84**, 255085 (2004).
[8]W. S. Ahn, W. W. Jung, S. K. Choi, and Y. Cho, Appl. Phys. Lett. **88**, 082902 (2006).
[9]A. Gruverman, H. Tokumoto, A. S. Prakash, S. Aggarwal, B. Yang, M. Wuttig, R. Ramesh, O. Auciello, and T. Venkatesan, Appl. Phys. Lett. **71**, 3492 (1997).
[10]A. Morelli, Sriram Venkatesan, G. Palasantzas, B. J. Kooi, and J. T. M. De Hosson, J. Appl. Phys. **102**, 084103 (2007).
[11]S. V. Kalinin and D. A. Bonnell, J. Mater. Res. **17**, 936 (2002).
[12]C. Harnagea, A. Pignolet, M. Alexe, D. Hesse, and U. Gösele, Appl. Phys. A: Mater. Sci. Process. **70**, 261 (2000).
[13]W. S. Ahn, S. H. Ahn, and S. K. Choi, J. Appl. Phys. **100**, 114118 (2006).
[14]S. A. Mabud and A. M. Glazer, J. Appl. Crystallogr. **12**, 49 (1979).
[15]C. W. Jones, P. D. Battle, P. Lightfoot, and W. T. A. Harrison, Acta Crystallogr., Sect. C: Cryst. Struct. Commun. **45**, 365 (1989).
[16]I. Vrejoiu, G. Le Rhun, L. Pintilie, D. Hesse, M. Alexe, and U. Gösele, Adv. Mater. (Weinheim, Ger.) **18**, 1657 (2006).
[17]Sriram Venkatesan, A. Vlooswijk, B. J. Kooi, A. Morelli, G. Palasantzas, B. Noheda, and J. Th. M. De Hosson, Phys. Rev. B **78**, 104112 (2008).
[18]V. V. Shvartsman, N. A. Pertsev, J. M. Herrero, C. Zaldo, and A. L. Kholkin, J. Appl. Phys. **97**, 104105 (2005).
[19]D. Damjanovic, J. Appl. Phys. **82**, 1788 (1997).
[20]Q. M. Zhang, H. Wang, N. Kim, and L. E. Cross, J. Appl. Phys. **75**, 454 (1994).
[21]T. Jungk, A. Hoffmann, and E. Soergel, Appl. Phys. A **86**, 353 (2007).
[22]V. V. Shvartsman, A. L. Kholkin, and N. A. Pertsev, Appl. Phys. Lett. **81**, 163025 (2002).
[23]S. Jesse, H. N. Lee, and S. V. Kalinin, Rev. Sci. Instrum. **77**, 073702 (2006).
[24]T. Morita and Y Cho, J. Korean Phys. Soc. **46**, 10 (2005).
[25]A. Gruverman and M. Tanaka, J. Appl. Phys. **89**, 1836 (2001).
[26]A. Morelli, G. Palasantzas, and J. T. M. De Hosson, J. Appl. Phys. **103**, 11 (2008).
[27]S. Trolier-McKinstry, N. Bassiri Gharb, and D. Damjanovic, Appl. Phys. Lett. **88**, 202901 (2006).